A Multifaceted Study of *Pseudomonas aeruginosa* Shutdown by Virulent Podovirus LUZ19

Rob Lavigne,[a] Elke Lecoutere,[a] Jeroen Wagemans,[a] William Cenens,[b] Abram Aertsen,[b] Liliane Schoofs,[c] Bart Landuyt,[c] Jan Paeshuyse,[d] Maurice Scheer,[e]* Max Schobert,[e] Pieter-Jan Ceyssens[a]

Division of Gene Technology, Katholieke Universiteit Leuven, Leuven, Belgium[a]; Centre for Food and Microbial Technology, Katholieke Universiteit Leuven, Heverlee, Belgium[b]; Animal Physiology and Neurobiology Section, Katholieke Universiteit Leuven, Leuven, Belgium[c]; Department of Microbiology and Immunology, Katholieke Universiteit Leuven, Leuven, Belgium[d]; Institute of Microbiology, Technical University of Braunschweig, Braunschweig, Germany[e]

* Present address: Maurice Scheer, The University Central Facility for Information and Communication Technology, Technische Universität Braunschweig, Braunschweig, Germany.

ABSTRACT **In contrast to the rapidly increasing knowledge on genome content and diversity of bacterial viruses, insights in intracellular phage development and its impact on bacterial physiology are very limited. We present a multifaceted study combining quantitative PCR (qPCR), microarray, RNA-seq, and two-dimensional gel electrophoresis (2D-GE), to obtain a global overview of alterations in DNA, RNA, and protein content in *Pseudomonas aeruginosa* PAO1 cells upon infection with the strictly lytic phage LUZ19. Viral genome replication occurs in the second half of the phage infection cycle and coincides with degradation of the bacterial genome. At the RNA level, there is a sharp increase in viral mRNAs from 23 to 60% of all transcripts after 5 and 15 min of infection, respectively. Although microarray analysis revealed a complex pattern of bacterial up- and downregulated genes, the accumulation of viral mRNA clearly coincides with a general breakdown of abundant bacterial transcripts. Two-dimensional gel electrophoretic analyses shows no bacterial protein degradation during phage infection, and seven stress-related bacterial proteins appear. Moreover, the two most abundantly expressed early and late-early phage proteins, LUZ19 gene product 13 (Gp13) and Gp21, completely inhibit *P. aeruginosa* growth when expressed from a single-copy plasmid. Since Gp13 encodes a predicted GNAT acetyltransferase, this observation points at a crucial but yet unexplored level of posttranslational viral control during infection.**

IMPORTANCE **Massive genome sequencing has led to important insights into the enormous genetic diversity of bacterial viruses (bacteriophages). However, for nearly all known phages, information on the impact of the phage infection on host physiology and intracellular phage development is scarce. This aspect of phage research should be revitalized, as phages evolved genes which can shut down or redirect bacterial processes in a very efficient way, which can be exploited towards antibacterial design. In this context, we initiated a study of the human opportunistic pathogen *Pseudomonas aeruginosa* under attack by one its most common predators, the *Phikmvlikevirus*. By analyzing various stages of infection at different levels, this study uncovers new features of phage infection, representing a cornerstone for future studies on members of this phage genus.**

Received 28 January 2013 **Accepted** 14 February 2013 **Published** 19 March 2013

Citation Lavigne R, Lecoutere E, Wagemans J, Cenens W, Aertsen A, Schoofs L, Landuyt B, Paeshuyse J, Scheer M, Schobert M, Ceyssens P-J. 2013. A multifaceted study of *Pseudomonas aeruginosa* shutdown by virulent podovirus LUZ19. mBio 4(2):e00061-13. doi:10.1128/mBio.00061-13.

Editor Anne Vidaver, University of Nebraska

Address correspondence to Rob Lavigne, rob.lavigne@biw.kuleuven.be.

The outcome of a virulent bacteriophage infection is determined by a complex struggle between the virus and the bacterial host during all stages of infection (1). After adsorbing to a susceptible host, the phage ejects its DNA into the bacterium and attempts to establish a favorable climate for phage production. This process occurs worldwide approximately 10^{23} times every second (2) and leads to a highly dynamic coevolutionary process of resistance and counterresistance in virus and host. Although this process is one of the major forces in microbial evolution (3), current knowledge of the impact of phage infection on host physiology is limited to a select number of (mainly) *Escherichia coli* phages. Well-known examples of these phage-host interactions are the transcriptional shutoff in *E. coli* by the Gp2 and Alc proteins of phages T7 and T4, respectively, or the cessation of DNA replication in *Staphylococcus aureus* through action of Gp104 of phage 77 (4–6).

This paper focuses on the intracellular development of the strictly lytic phage LUZ19 infecting *Pseudomonas aeruginosa* PAO1, an isolate of the *Pseudomonas* phage phiKMV (7). This podovirus carries a 43,548-bp genome, which is delineated by long direct terminal repeats. It contains 54 predicted genes organized in clusters of early, middle, and late expression. The genome is over 90% identical to other members of the *Phikmvlikevirus* genus, which is a genus of extremely abundant *Pseudomonas* phages which can be readily isolated from wastewaters around the world (8). These phages belong to the family of the *Autographivirinae*, as

they encode their own single-subunit RNA polymerase (RNAP), relying on the transcriptional apparatus of the host only for transcription of the early and middle genes (9).

The host organism in this study, *P. aeruginosa* PAO1, is a bacterium with extreme metabolic versatility. It is able to colonize various environmental habitats and to persist and grow under nutrient-poor and hostile conditions (10). *P. aeruginosa* can switch from a soil and water organism to an opportunistic human pathogen and is responsible for life-threatening infections in cystic fibrosis and burn wound patients (11). The extraordinary physiological capacities of this Gram-negative bacterium have been studied intensively, mainly by using the available *P. aeruginosa* GeneChip (Affymetrix) to analyze differential gene expression (e.g., see references 12 to 14).

In this study, we combine quantitative PCR (qPCR), microarray, RNA-seq, and two-dimensional gel electrophoresis (2D-GE) proteome methods in the study of the global effect of LUZ19 infection on host physiology. By analyzing different stages of infection, we gather insights into viral transcriptional overtake and stress responses provoked in the host and show the influence of a virulent phage infection on the DNA, RNA, and protein content of *P. aeruginosa*.

RESULTS

Characterization of LUZ19 infection. To analyze phage-host interplay at various stages of infection, we first studied the gross infection parameters of LUZ19. Exponentially growing *P. aeruginosa* cells were infected at an OD at 600 nm (OD_{600}) of 0.3 (1.2×10^8 CFU/ml). Stepwise increasing amounts of phages added to these cultures clearly showed that a single infection cycle is completed in approximately 24 min and that addition of a 10-fold excess of phages leads to coordinated cell death after one generation. Moreover, within the first minute after phage addition, a 4-log reduction in nonadsorbed phage particles was observed ($k_a = 3.34 \times 10^{-7}$ ml min^{-1}), which is indicative of synchronized infected cultures (see Fig. S1 in the supplemental material). For all further experiments, a 10-fold excess of phages over bacteria was used.

Viral DNA amplification initiates after 14 min. Phage LUZ19 encodes a replication cluster which closely resembles the well-studied phage T7 replisome and initiates genome amplification 6 min after the onset of infection (8, 15, 16). To study the timing of genome replication and the fate of *P. aeruginosa* DNA during LUZ19 infection, we extracted total DNA from infected cells at 5- to 7-min intervals. Next, we determined the abundance of genomic copies of gene 19 (phage) and three bacterial reporter genes, *oprL*, *lppL*, and PA3326, by quantitative PCR. In this experiment, we observed that LUZ19 genome replication starts only after 14 min of infection. Host DNA replication is not shut down before this time point, as the copy number of the selected genes doubles compared to that at the moment of infection (Fig. 1; see also Fig. S2 and S3 in the supplemental material). However, coinciding with phage genome amplification, the bacterial genome is degraded, presumably providing the phage with nucleotide building blocks (Fig. 1A). As this degradation is observed for the three distantly carried bacterial reporter genes, it more than likely represents a genome-wide phenomenon. Analogous to phage T7 (17), this breakdown of the host chromosome is probably mediated by the combined action of the 5′ to 3′ exonuclease (gene 22) and the type 7 endonuclease (gene 23), which are encoded among

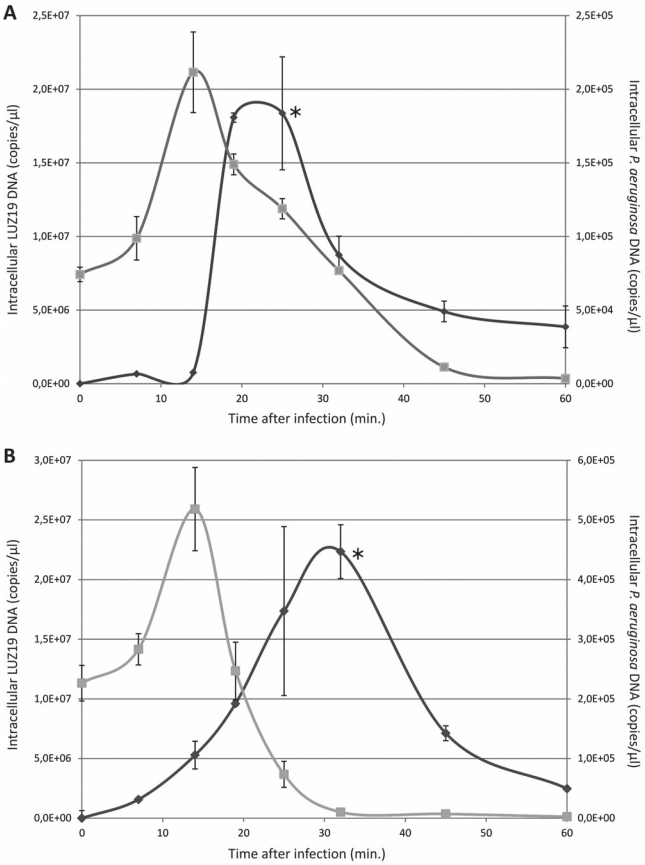

FIG 1 qPCR analysis of LUZ19-infected *P. aeruginosa* cells in LB medium (A) and M9 minimal medium (B). Cellular DNA was extracted at regular intervals, and the quantity of genes 19 (LUZ19, black line) and *oprL* (*P. aeruginosa*, gray line) over time was monitored in three independent reactions. The moment of lysis is indicated with an asterisk. The results obtained for two other bacterial reporter genes (*llpL* and PA3326) are shown in Fig. S3 in the supplemental material.

the DNA replication genes of LUZ19. In LB medium, approximately half of the *P. aeruginosa* PAO1 genome is degraded at the end of the infection cycle. Interestingly, the entire host chromosome is broken down at the moment of cell lysis when this experiment is performed in M9 minimal medium (Fig. 1B).

Transcript isolation and sequencing. In a next step, we analyzed changes in the cellular RNA content provoked by phage infection. In two independent experiments, total cellular RNA was extracted immediately before and after 5 and 15 min of phage infection. rRNAs were depleted by subtractive hybridization, and mRNA samples were checked for integrity by an Agilent Bioanalyzer. These samples were subjected to both classical microarray (Affymetrix) and RNA-seq analysis. In the latter analysis, between 16 and 51 million reads of more than 20 bases were generated, resulting in the sequencing of 780 to 2,396 million bases in total (see Table S1 in the supplemental material). By iterative alignment and 3′-end trimming, on average 88.5% of the reads could be mapped to either the bacterial or the phage genome. Although we performed subtractive hybridization to remove bacterial rRNAs as described in Materials and Methods (18), the majority of sequence reads (up to 98%) still represented rRNAs and other structural RNAs. This inability to successfully extract rRNAs from *P. aerugi-*

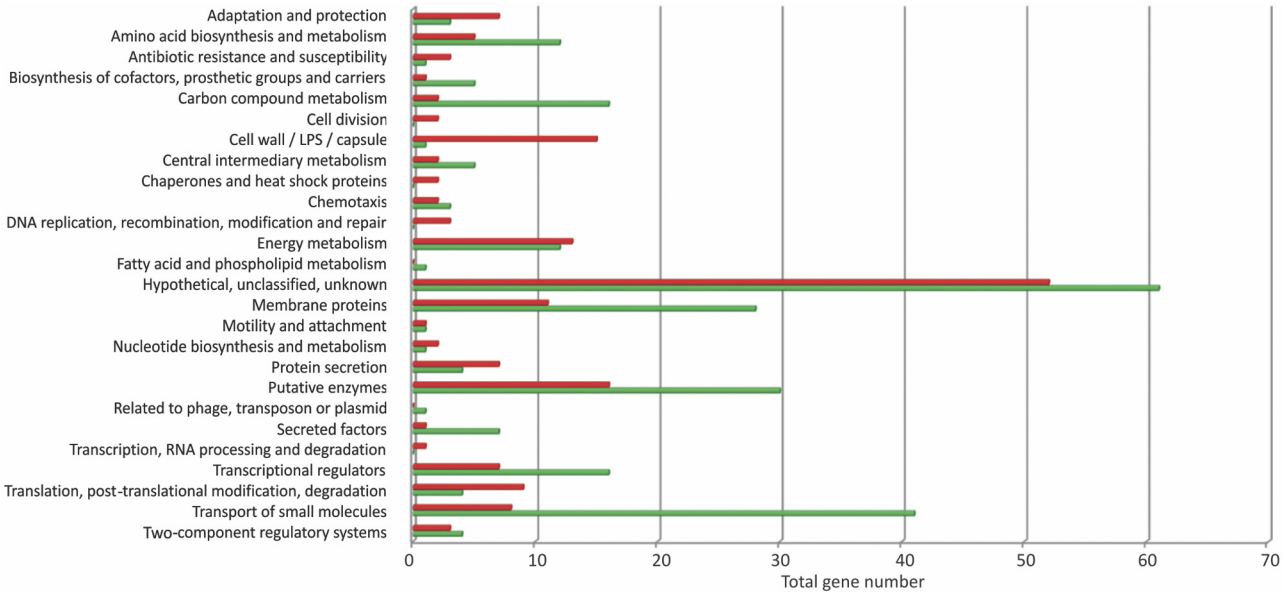

FIG 2 Differential expression of *P. aeruginosa* genes after LUZ19 infection. Depicted are the total number of genes which displayed a minimal 2-fold up- or downregulation (green and red, respectively) in the microarray study, categorized according to the work of Stover et al. (21).

nosa total RNA by this method was recently also reported by Dötsch et al. (19).

Influence of phage infection on bacterial gene expression. The microarray analysis showed that 220 *P. aeruginosa* genes are relatively upregulated during LUZ19 infection (posterior probability of differential expression [PPDE], >0.95). This is distinctly different from other lytic phage-host systems where few, if any, host genes become activated (17, 20). Moreover, 13 operons were coordinately downregulated, also suggesting targeted shutdown of transcription (Fig. 2; see also Table S2 in the supplemental material). By classifying these genes in various functional groups (21), we observed that 25 significantly regulated genes are directly classified as energy metabolism genes. However, many more are indirectly linked to the energy status of the cell, such as enzymes and other macromolecule metabolism genes. Two of the most highly induced genes, *glyA1* (+4.97) and *hutU* (+4.02), for instance, play an important role in amino acid metabolism. Another striking observation is the rapid downregulation of the *nuo* gene cluster, encoding the NADH dehydrogenase complex, and the repression of the cytochrome *o* ubiquinol oxidase subunits.

Also notable are the changes in gene expression of various membrane-related genes. For example, the *wbp* and *arn* operons, which mediate the biosynthesis of the lipopolysaccharide (LPS) O antigen and lipid A layer, respectively, are strongly downregulated during phage infection. Moreover, three type IV pilus genes, whose products serve as primary receptors for LUZ19 (22), are repressed. We refer to the supplemental material for a detailed overview and discussion of all differentially expressed genes and operons.

Instability of abundant bacterial transcripts. Two major advantages of RNA-seq over the GeneChip array data are that it allows identification of phage transcripts and estimation of transcript abundance. In comparing the total amounts of nonstructural RNA reads originating from phage and bacteria from our RNA-seq data, we observed a steep increase from 23.6 to 60.2% of phage mRNA after 5 and 15 min of infection, respectively. As this increase could be caused by both rapid phage transcription and host mRNA degradation, we analyzed the RNA-seq data sets for differential gene expression with two algorithms, edgeR and DESeq (23, 24) at the default false discovery rate of 0.1 (25) (Fig. 3A). For the bulk of the bacterial transcripts, no obvious degradation was observed; 49 and 52% of them were at least as abundant after 5 and 15 min of infection, respectively, as in the uninfected sample. However, it is clear that the most abundant host transcripts are degraded when the phage infection proceeds, except for a few (conserved) hypothetical gene transcripts: PA4463, PA3623, PA4323, PA0257, and PA0689 (Fig. 3A). The abundant transcripts on the right end of the graph represent rRNA, which appears unaffected by LUZ19 infection.

Phage transcription. Using a pile-up of all RNA sequence reads of phage transcripts, we visualized the genome coverage at two points during infection. This profile shows the expected shift in transcripts from early to late genes after 5 and 15 min of infection, respectively, indicative of the temporal pattern of gene expression (Fig. 3B). Moreover, a characteristic enrichment of sequence reads in promoter regions is observed. This phenomenon arises as the 5′ end of a transcript is always present in the leftmost fragment after random fragmentation. As such, independently of the exact fragmentation point, reads which originate from the transcript left ends are overrepresented (19).

Early transcription is clearly initiated from three promoters at positions 913, 1147, and 1248 in front of the first gene. These promoters strongly resemble the bacterial σ^{70} consensus sequence (TTGACA at the −35 box, TAcAAg at −10). The second viral transcriptional profile, generated after 15 min of infection, showed various sharp peaks throughout the genome. The majority of these correspond to intergenic region upstream genes 23, 27 (downstream of the RNA polymerase gene), 32 (capsid protein), and 37, 42, and 47 (head decoration proteins). Although one could hypothesize that these transcripts originate from virus-

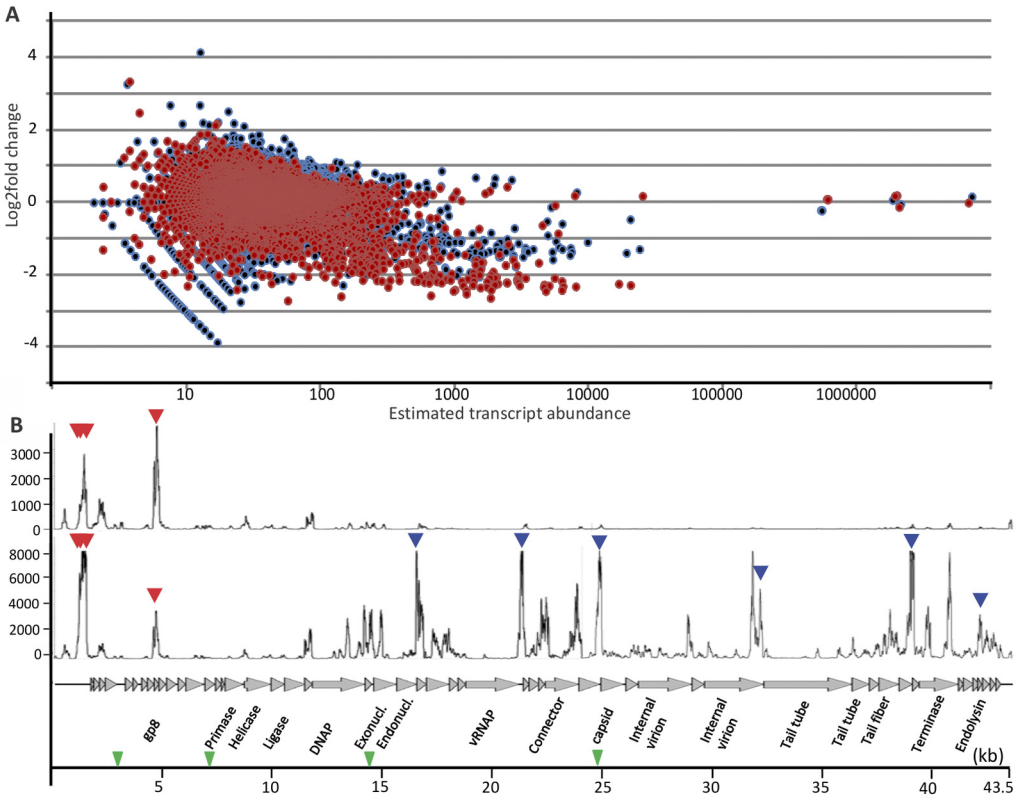

FIG 3 Analysis of the RNA-seq data. (A) Differential expression in *P. aeruginosa* genes by DESeq analysis of gene counts at a false discovery rate of 0.1. Each dot represents a specific gene after 5 (blue) and 15 (red) minutes of LUZ19 infection, with its estimated transcript abundance on the *x* axis and its $\log_2$ fold change compared to the uninfected sample on the *y* axis. The dots on the right end of the graph represent rRNAs. (B) Pile-up of LUZ19 reads after 5 (top graph) and 15 (bottom graph) minutes of infection. The intergenic regions which are presumably associated with host- and phage-specific promoters are indicated with red and blue triangles, respectively. The locations of single-stranded interruptions on the noncoding strand as defined by Kulakov et al. (26) are shown as green triangles.

specific RNA polymerase, no common promoter motif could be detected at these sites. The only detectable intergenic motif (CCT ACTCCGG) at positions 3132, 6755, 14415, and 24767 was previously associated with localized, single-stranded nicks on the noncoding strand (26). However, no relation to transcript abundance is apparent (Fig. 3B).

Subtle changes in bacterial proteome after phage LUZ19 infection. In a next step, we compared 2D-PAGE cytoplasmic proteome maps of exponentially growing, uninfected *P. aeruginosa* PAO1 cells to corresponding maps of cells after infection with LUZ19. The reference map of uninfected *P. aeruginosa* cells contained (on average) 1,128 spots per 200 μg of cell lysate and was recently published by our group (27). Using similar techniques, three phage infection maps were created at 5-min intervals, giving a spread of analysis points during the entire phage cycle (see Fig. S4 in the supplemental material). By comparing the 2D maps, it is apparent that the global impact of phage infection on the host proteome is limited. With only one exception (see below), we did not detect protein modifications that alter the protein mass or isoelectric point. Moreover, almost no degradation of host proteins was observed. In the pI range of 4 to 7, 12 new spots were detected during infection and identified using electrospray ionization-tandem mass spectrometry (ESI–MS-MS). Six of these represented host proteins are involved in stress responses (PasP protease, PA2807, and AotJ), energy metabolism (SdhB), and translation (EF-Tu and RplL). An intriguing observation concerns RpoA (PA4238), the alpha subunit of the bacterial RNA polymerase (RNAP). In the noninfected sample, two isoforms of this protein were detected, both with an estimated protein mass of 44 kDa. LUZ19 infection induced a shift of this spot to a molecular mass of approximately 32 kDa, indicative of degradation upon phage infection or sample preparation. We refer to the supplemental material for a detailed discussion of these proteins.

Appearance of abundant phage proteins. At distinct time points during infection, five LUZ19 proteins were detected on the two-dimensional electrophoresis (2-DE) infection maps. They belong to different gene classes (early, middle, and late) and again illustrate the timed regulation of phage infection. First, a highly abundant early protein (Gp10) appeared (Fig. 4, inset). Shortly thereafter, two late-early/middle proteins, Gp13 and Gp21, were detected. Based on the location of the protein spot in the 2D gel and identified peptides during mass spectrometry, the gene annotation of Gp13 was reevaluated (see the supplemental material). The most abundant phage protein was, as expected, the major capsid protein Gp32, which appeared first after 10 min of infection and increased in abundance in the course of the phage infection. The putative tail fiber Gp41 was also identified. Other phage proteins either were too small to be detected, were not abundant enough, or fell outside our pI range.

Based on sequence similarity, the function of Gp10 and Gp21

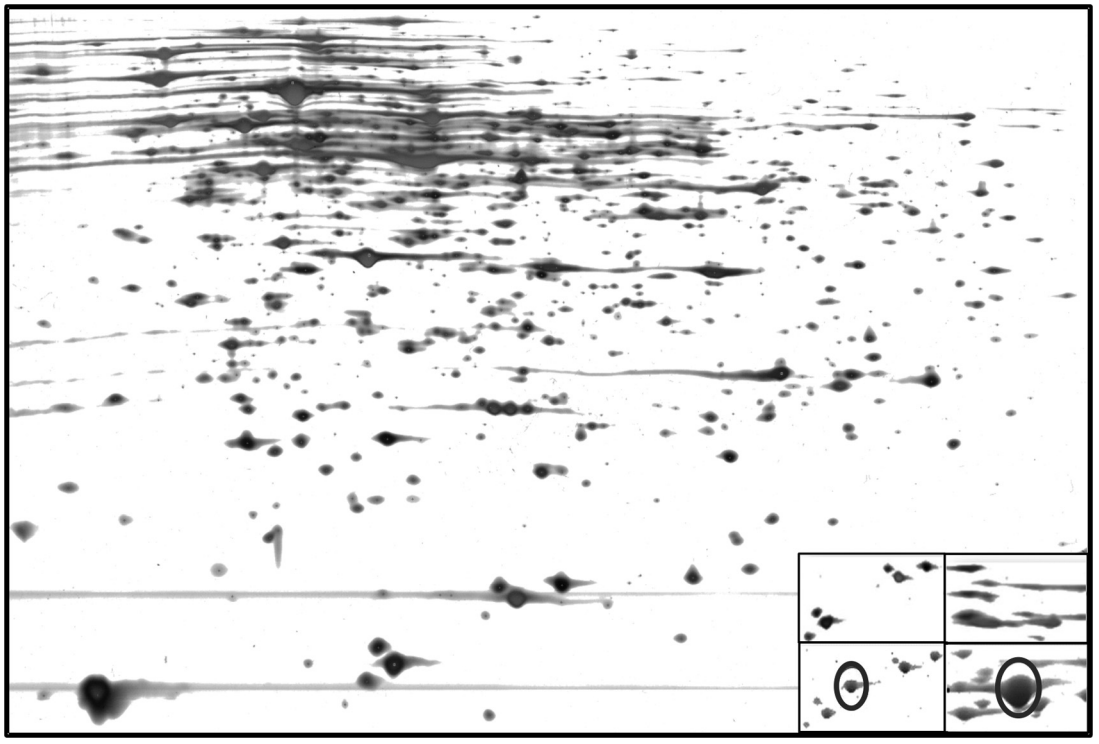

FIG 4 Two-dimensional proteome map of *P. aeruginosa* cells, 5 min after infection with LUZ19. The right corner shows outtakes of two corresponding gel regions from the uninfected sample (upper panel) and after 5 and 15 min of infection, respectively (lower panel). The encircled spots were identified as LUZ19 Gp10 (left) and the major phage capsid protein Gp32 (right).

cannot be predicted, although the latter is conserved in many podoviruses and prophages (PHA02030, $E = 2.1 \times e^{-151}$). In contrast, Gp13 is highly similar to various bacterial GNAT acetyltransferases (pfam13508, $E = 2.51 \times e^{-8}$). To gain insight into the individual impact of these abundant early phage proteins on host physiology, they were cloned in a single-copy pUC18-mini-Tn7T-LAC expression vector (28) which integrates into the bacterial genome (Fig. 5A), and cell growth was monitored upon induction. Interestingly, while Gp10 had no influence on *P. aeruginosa* growth, expression of both Gp13 and Gp21 was sufficient to block bacterial growth completely in both solid and liquid media (Fig. 5B). Time-lapse microscopic recordings of these cells showed that the presence of the phage acetyltransferase slows bacterial growth down, while Gp21 expression leads to an immediate growth arrest (Fig. 5C; see also movies M1 to M3 in the supplemental material). Given that Gp21 is encoded among genes involved in DNA replication and directly precedes the phage-encoded exo- and endonucleases, we explored the possibility that this protein is involved in shutdown of bacterial DNA replication. Therefore, we followed the incorporation of radiolabeled macromolecular precursors in *P. aeruginosa* cells with and without induction. For Gp21, we observed an immediate drop of 20 to 25% in transcription and translation. However, DNA replication seemed unaffected (Fig. 5D). In contrast, translation appears unaffected in the first 30 min after Gp13 induction, while DNA replication and transcription levels decrease approximately 30% compared to those in noninduced *P. aeruginosa* cells. Only 21% residual transcriptional activity is remaining after 65 min of Gp13 induction (Fig. 5D). The elucidation of the binding partner(s) and working mechanisms of these proteins is under investigation.

DISCUSSION

In this paper, we describe a study of the total DNA, RNA, and cytoplasmic protein content of phage-infected *P. aeruginosa* PAO1 cells based on qPCR analyses, whole-cell proteomics, and transcriptome analyses by both microarray and RNA-seq technology. We selected the obligatory lytic podovirus LUZ19 for this analysis, which adsorbs rapidly to the host cell and completes its infection cycle within 25 min. Early bacteriophage transcription could be clearly associated with three promoters directly upstream of gene 1, which closely resembles the σ^{70} consensus sequence. Later in infection, many potential transcriptional start sites could be detected alongside the phage genome, but no LUZ19-specific promoter consensus sequence could be retrieved. Due to the method of cDNA library construction (see the supplemental material), no information on antisense transcripts could be inferred. In the future, directional transcriptome maps for this (and other) phages can be generated by constructing libraries from first-strand cDNA (29).

A clear observation was the rapid accumulation of phage transcripts during LUZ19 infection, in contrast to breakdown of bacterial mRNA. Experiments presented in this study clearly show that this breakdown initiates before bacterial genome replication arrests. There is certainly an advantage for a virulent phage to accelerate host mRNA degradation immediately after infection, as this contributes to making the translation apparatus more rapidly available for viral mRNAs and facilitates the transition from the host to phage gene expression (30). In the related coliphage T7, the protein kinase Gp0.7 phosphorylates the C-terminal domain of RNase E, which protects T7 mRNA from degradation (31). As no

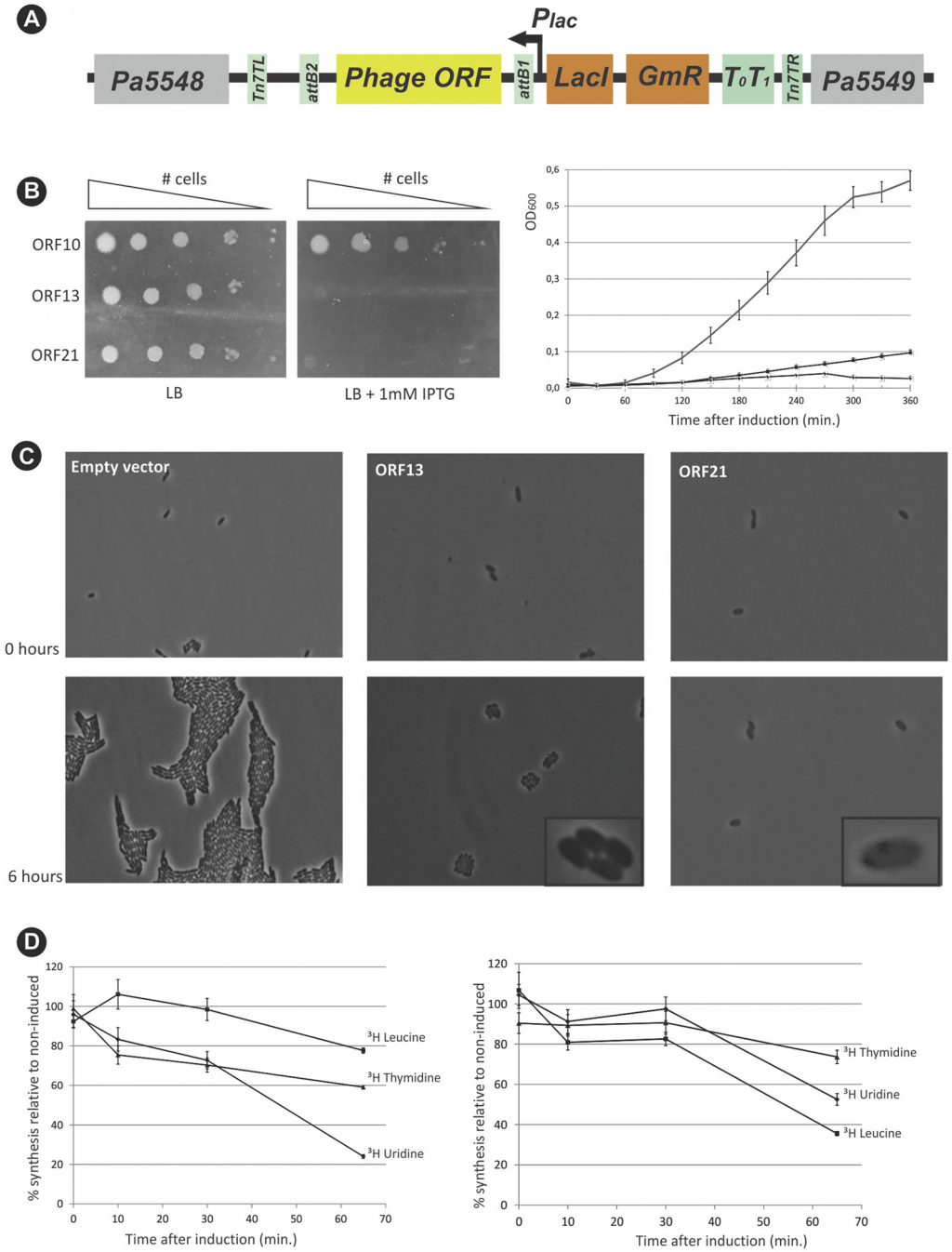

FIG 5 Analysis of phenotypic effects provoked by LUZ19 genes 10, 13, and 21 on *P. aeruginosa* PAO1. (A) The three genes were stably incorporated in single copy in the bacterial genome through Tn*7*-mediated integration of the expression vector pUC18-mini-Tn7T-LAC. ORF, open reading frame. (B) Phenotypic effect of phage gene expression on bacterial growth on solid (left) and in liquid (right) (gray line, empty vector; squares, Gp13; dots, Gp21) LB media supplemented with 1 mM isopropyl-β-D-thiogalactopyranoside (IPTG). (C) Time-lapse screen shots of a bacterial culture at the moment of gene induction (upper pictures) and after 6 h of induction at 37°C (bottom pictures). (D) Incorporation of radioactively labeled [^{3}H]uridine, [^{3}H]leucine, and [^{3}H]thymidine, followed in time upon induction of Gp13 (left panel) and Gp21 (right panel). All experiments were performed in triplicate; standard deviations are indicated on the graphs.

homologue to the T7 kinase is encoded in LUZ19, we speculate on another type of modulation of the host degradosome.

It is possible that LUZ19 exerts posttranslational control by acetylation instead of phosphorylation. The early phage protein Gp13 is an acetyltransferase for which we showed that single-copy expression is detrimental for *P. aeruginosa* and hinders both DNA replication and transcription. These types of enzymes are recognized more and more as serving pivotal roles in the posttranslational control of central microbial metabolism and are reported to be able to modulate enzyme activity (32, 33). Phage-induced acet-

ylation of specific phage or host proteins has not been reported thus far, and the study of the targets of Gp13 is a very interesting area of future research.

Even though virulent phage infection has a clear impact on the cellular RNA content, only moderate changes were observed at the protein level. This is not unexpected, as the average half-life of bacterial proteins exceeds the time span of the phage infection (34). Possible host transcription shutdown or bacterial mRNA degradation would in this case not result in a decrease of protein spots on 2-DE gels. We observed significant upregulation of a small number of proteins which previously have been shown to be associated with stress, like the EF-Tu elongation factor and the 50S ribosomal protein RplL (35, 36). In addition, a notable result from this study was the observed mass shift in the alpha subunit of the RNA polymerase during phage infection. All bacteriophages known so far redirect the bacterial RNAP toward transcription of the viral genome. While the majority of them recruit the host RNAP throughout the infection cycle, some phages (like LUZ19, T7, and N4) encode their own RNAP and rely on the host's machinery only for transcription of early or late genes (17, 37). For this molecular hijacking, two main types of phage-induced modifications have been described so far: covalent RNAP modifications and modifications through RNAP-binding proteins (38). This observation could represent an entirely novel mechanism of viral control over the host transcriptional apparatus.

MATERIALS AND METHODS

Unless stated otherwise, *Pseudomonas aeruginosa* PAO1 cells grown in LB medium were used for all experiments. Inducible single-copy expression of phage genes was achieved by integration of the target gene under a *lac* promoter into the bacterial genome using the pUC18-mini-Tn7T-LAC and pTNS2 suicide plasmids (28). High-titer phage stocks of LUZ19 were purified using two consecutive CsCl gradient centrifugations.

For the transcriptome analyses, total RNA from phage-infected cells was isolated from the bacteria by a modified hot-phenol method in combination with the RNeasy midikit (Qiagen, Hilden, Germany). rRNA was extracted by hybridization to antisense oligonucleotides, followed by pull-down through binding by magnetic beads (MicrobExpress kit; Ambion). Subsequent cDNA library constructions for microarray and RNA-seq analysis were based on standard protocols for the Affymetrix *Pseudomonas* GeneChip and Illumina HISeq2000 sequencing, respectively. Array analyses were carried out using R and Bioconductor, and the preprocessed expression data were analyzed by a regularized *t* test based on a Bayesian statistical framework using the CyberT algorithm. The raw sequence data were checked for quality and mapped to the *P. aeruginosa* PAO1 (NC_002516.2) and LUZ19 (NC_010326.1) reference genomes using Bowtie (39). Count data were analyzed for differential gene expression using the DEB web interface.

The proteome analysis was performed by halting the LUZ19 infection at 5-min intervals and performing two-dimensional electrophoresis (2-DE) separations and image analyses on clear cell lysates. 2-DE gels were silver stained, and image acquisition was performed using a calibrated flatbed ImageScanner, combined with LabScan software according to the manufacturer's protocols. 2-DE maps were analyzed, and spot data were generated by standard spot detection parameters using ImageMaster 2D platinum software. Differential spots were picked and identified using ESI–MS-MS.

Detailed procedures can be found in the supplemental material.

SUPPLEMENTAL MATERIAL

Supplemental material for this article may be found at http://mbio.asm.org/lookup/suppl/doi:10.1128/mBio.00061-13/-/DCSupplemental.

Text S1, DOCX file, 0.1 MB.
Figure S1, PDF file, 0.2 MB.
Figure S2, PDF file, 0.2 MB.
Figure S3, PDF file, 0.2 MB.
Figure S4, PDF file, 0.7 MB.
Table S1, DOCX file, 0.1 MB.
Table S2, DOCX file, 0.1 MB.
Movie M1, MOV file, 1.7 MB.
Movie M2, MOV file, 1.5 MB.
Movie M3, MOV file, 1.7 MB.

ACKNOWLEDGMENTS

P. J. Ceyssens is a Postdoctoral Fellow of the Research Foundation of Flanders (FWO-Vlaanderen). Jeroen Wagemans is a predoctoral research fellow supported by the Agentschap voor Innovatie door Wetenschap en Technologie (IWT) of the Flemish Government. This research was supported by grant G.0323.09 from the FWO, SBO project 100042 of the IWT, and the CREA/09/017 grant of the KU Leuven Research Fund.

We thank Annika Steen for assistance with microarray analysis.

REFERENCES

1. **Labrie SJ, Samson JE, Moineau S.** 2010. Bacteriophage resistance mechanisms. Nat. Rev. Microbiol. **8**:317–327.
2. **Suttle CA.** 2007. Marine viruses—major players in the global ecosystem. Nat. Rev. Microbiol. **5**:801–812.
3. **Gómez P, Buckling A.** 2011. Bacteria-phage antagonistic coevolution in soil. Science **332**:106–109.
4. **Kashlev M, Nudler E, Goldfarb A, White T, Kutter E.** 1993. Bacteriophage T4 Alc protein: a transcription termination factor sensing local modification of DNA. Cell **75**:147–154.
5. **Nechaev S, Severinov K.** 1999. Inhibition of Escherichia coli RNA polymerase by bacteriophage T7 gene 2 protein. J. Mol. Biol. **289**:815–826.
6. **Liu J, Dehbi M, Moeck G, Arhin F, Bauda P, Bergeron D, Callejo M, Ferretti V, Ha N, Kwan T, McCarty J, Srikumar R, Williams D, Wu JJ, Gros P, Pelletier J, DuBow M.** 2004. Antimicrobial drug discovery through bacteriophage genomics. Nat. Biotechnol. **22**:185–191.
7. **Lavigne R, Burkal'tseva MV, Robben J, Sykilinda NN, Kurochkina LP, Grymonprez B, Jonckx B, Krylov VN, Mesyanzhinov VV, Volckaert G.** 2003. The genome of bacteriophage phiKMV, a T7-like virus infecting *Pseudomonas aeruginosa*. Virology **312**:49–59.
8. **Ceyssens PJ, Glonti T, Kropinski NM, Lavigne R, Chanishvili N, Kulakov L, Lashkhi N, Tediashvili M, Merabishvili M.** 2011. Phenotypic and genotypic variations within a single bacteriophage species. Virol. J. **8**:134. http://dx.doi.org/10.1186/1743-422X-8-134.
9. **Kropinski AM, Prangishvili D, Lavigne R.** 2009. Position paper: the creation of a rational scheme for the nomenclature of viruses of Bacteria and Archaea. Environ. Microbiol. **11**:2775–2777.
10. **Schmidt KD, Tümmler B, Römling U.** 1996. Comparative genome mapping of *Pseudomonas aeruginosa* PAO with *P. aeruginosa* C, which belongs to a major clone in cystic fibrosis patients and aquatic habitats. J. Bacteriol. **178**:85–93.
11. **Mann EE, Wozniak DJ.** 2012. Pseudomonas biofilm matrix composition and niche biology. FEMS Microbiol. Rev. **36**:893–916.
12. **Palma M, DeLuca D, Worgall S, Quadri LE.** 2004. Transcriptome analysis of the response of *Pseudomonas aeruginosa* to hydrogen peroxide. J. Bacteriol. **186**:248–252.
13. **Aspedon A, Palmer K, Whiteley M.** 2006. Microarray analysis of the osmotic stress response in *Pseudomonas aeruginosa*. J. Bacteriol. **188**:2721–2725.
14. **Chen SH, Chen RY, Xu XL, Xiao WB.** 2012. Microarray analysis and phenotypic response of *Pseudomonas aeruginosa* PAO1 under hyperbaric oxyhelium conditions. Can. J. Microbiol. **58**:158–169.
15. **Lee SJ, Richardson CC.** 2011. Choreography of bacteriophage T7 DNA replication. Curr. Opin. Chem. Biol. **15**:580–586.
16. **Serwer P, Watson RH, Son M.** 1990. Role of gene 6 exonuclease in the replication and packaging of bacteriophage T7 DNA. J. Mol. Biol. **215**:287–299.
17. **Molineux IJ.** 2006. The T7 group, p 277–301. *In* Calendar R (ed), The bacteriophages. Oxford University Press, New York, NY.
18. **He S, Wurtzel O, Singh K, Froula JL, Yilmaz S, Tringe SG, Wang Z, Chen F, Lindquist EA, Sorek R, Hugenholtz P.** 2010. Validation of two

ribosomal RNA removal methods for microbial metatranscriptomics. Nat. Methods **7**:807–812.
19. **Dötsch A, Eckweiler D, Schniederjans M, Zimmermann A, Jensen V, Scharfe M, Geffers R, Häussler S.** 2012. The *Pseudomonas aeruginosa* transcriptome in planktonic cultures and static biofilms using RNA sequencing. PLoS One **7**:e31092. http://dx.doi.org/10.1371/journal.pone.0031092.
20. **Lindell D, Jaffe JD, Coleman ML, Futschik ME, Axmann IM, Rector T, Kettler G, Sullivan MB, Steen R, Hess WR, Church GM, Chisholm SW.** 2007. Genome-wide expression dynamics of a marine virus and host reveal features of co-evolution. Nature **449**:83–86.
21. **Stover CK, Pham XQ, Erwin AL, Mizoguchi SD, Warrener P, Hickey MJ, Brinkman FS, Hufnagle WO, Kowalik DJ, Lagrou M, Garber RL, Goltry L, Tolentino E, Westbrock-Wadman S, Yuan Y, Brody LL, Coulter SN, Folger KR, Kas A, Larbig K, Lim R, Smith K, Spencer D, Wong GK, Wu Z, Paulsen IT, Reizer J, Saier MH, Hancock RE, Lory S, Olson MV.** 2000. Complete genome sequence of *Pseudomonas aeruginosa* PAO1, an opportunistic pathogen. Nature **406**:959–964.
22. **Chibeu A, Ceyssens PJ, Hertveldt K, Volckaert G, Cornelis P, Matthijs S, Lavigne R.** 2009. The adsorption of *Pseudomonas aeruginosa* bacteriophage phiKMV is dependent on expression regulation of type IV pili genes. FEMS Microbiol. Lett. **296**:210–218.
23. **Robinson MD, McCarthy DJ, Smyth GK.** 2010. edgeR: a bioconductor package for differential expression analysis of digital gene expression data. Bioinformatics **26**:139–140.
24. **Anders S, Huber W.** 2010. Differential expression analysis for sequence count data. Genome Biol. **11**:R106. http://dx.doi.org/10.1186/gb-2010-11-10-r106.
25. **Yao JQ, Yu F.** 2011. DEB: a web interface for RNA-seq digital gene expression analysis. Bioinformation **7**:44–45.
26. **Kulakov LA, Ksenzenko VN, Shlyapnikov MG, Kochetkov VV, Del Casale A, Allen CC, Larkin MJ, Ceyssens PJ, Lavigne R.** 2009. Genomes of "phiKMV-like viruses" of *Pseudomonas aeruginosa* contain localized single-strand interruptions. Virology **391**:1–4.
27. **Lecoutere E, Verleyen P, Haenen S, Vandersteegen K, Noben JP, Robben J, Schoofs L, Ceyssens PJ, Volckaert G, Lavigne R.** 2012. A theoretical and experimental proteome map of *Pseudomonas aeruginosa* PAO1. MicrobiologyOpen **1**:169–181.
28. **Choi KH, Gaynor JB, White KG, Lopez C, Bosio CM, Karkhoff-Schweizer RR, Schweizer HP.** 2005. A Tn7-based broad-range bacterial cloning and expression system. Nat. Methods **26**:443–448.
29. **Høvik H, Yu WH, Olsen I, Chen T.** 2012. Comprehensive transcriptome analysis of the periodontopathogenic bacterium Porphyromonas gingivalis W83. J. Bacteriol. **194**:100–114.
30. **Uzan M.** 2009. RNA processing and decay in bacteriophage T4. Prog. Mol. Biol. Transl. Sci. **85**:43–89.
31. **Marchand I, Nicholson AW, Dreyfus M.** 2001. Bacteriophage T7 protein kinase phosphorylates RNase E and stabilizes mRNAs synthesized by T7 RNA polymerase. Mol. Microbiol. **42**:767–776.
32. **Hu LI, Lima BP, Wolfe AJ.** 2010. Bacterial protein acetylation: the dawning of a new age. Mol. Microbiol. **77**:15–21.
33. **Thao S, Escalante-Semerena JC.** 2011. Control of protein function by reversible Nε-lysine acetylation in bacteria. Curr. Opin. Microbiol. **14**:200–204.
34. **Picard F, Dressaire C, Girbal L, Cocaign-Bousquet M.** 2009. Examination of post-transcriptional regulations in prokaryotes by integrative biology. C. R. Biol. **332**:958–973.
35. **Leverrier P, Vissers JP, Rouault A, Boyaval P, Jan G.** 2004. Mass spectrometry proteomic analysis of stress adaptation reveals both common and distinct response pathways in Propionibacterium freudenreichii. Arch. Microbiol. **181**:215–230.
36. **Jofré A, Champomier-Vergès M, Anglade P, Baraige F, Martin B, Garriga M, Zagorec M, Aymerich T.** 2007. Protein synthesis in lactic acid and pathogenic bacteria during recovery from a high pressure treatment. Res. Microbiol. **158**:512–520.
37. **Cho NY, Choi M, Rothman-Denes LB.** 1995. The bacteriophage N4-coded single-stranded DNA-binding protein (N4SSB) is the transcriptional activator of Escherichia coli RNA polymerase at N4 late promoters. J. Mol. Biol. **246**:461–471.
38. **Nechaev S, Severinov K.** 2008. The elusive object of desire—interactions of bacteriophages and their hosts. Curr. Opin. Microbiol. **11**:186–193.
39. **Langmead B, Trapnell C, Pop M, Salzberg SL.** 2009. Ultrafast and memory-efficient alignment of short DNA sequences to the human genome. Genome Biol. **10**:R25. http://dx.doi.org/10.1186/gb-2009-10-3-r25.